CHEMISTRY
A European Journal

Accepted Article

Title: Unexpected importance of aromatic-aliphatic and aliphatic side chain-backbone interactions in the stability of amyloids

Authors: Dragan B. Ninković, Dušan P. Malenov, Predrag V. Petrović, Edward N. Brothers, Shuqiang Niu, Michael B. Hall, Milivoj R. Belić, and Snežana D. Zarić

WILEY-VCH

FULL PAPER

WILEY-VCH

Unexpected importance of aromatic-aliphatic and aliphatic side chain-backbone interactions in the stability of amyloids

Dragan B. Ninković,[a, c] Dušan P. Malenov,[b] Predrag V. Petrović,[a, c] Edward N. Brothers,[a] Shuqiang Niu,[d] Michael B. Hall,[d] Milivoj R. Belić,[a] and Snežana D. Zarić*[a, b]

Abstract: The role of aromatic and nonaromatic amino acids in amyloid formation was elucidated by calculating interaction energies between β-sheets in amyloid model systems using density functional theory (B3LYP-D3/6-31G*). The model systems were based on experimental crystal structures of two types of amyloids: (1) with aromatic amino acids and (2) without aromatic amino acids. Data show that these two types of amyloids have similar interaction energies, supporting experimental findings that aromatic amino acids are not essential for amyloid formation. However, different factors contribute to the stability of these two types of amyloids. On one hand, in (1) presence of aromatic amino acids contribute significantly to the strength of interactions between side chains; interactions between aromatic and aliphatic side chains are the strongest, followed by aromatic-aromatic interactions, while aliphatic-aliphatic interactions are the weakest. On the other hand, stability of amyloids (2), without aromatic residues, is caused by interactions of aliphatic side chains with the backbone and, in some cases, by hydrogen bonds.

Introduction

Amyloid fibrils have been associated with the pathology of more than 20 serious human diseases, including various neurodegenerative disorders such as Alzheimer's and Parkinson's diseases.[1] Although the frequent occurrence of aromatic residues in natural amyloids led to the belief that aromatic amino acids play an important role in amyloid fibril formation,[2-10] the central role of aromatic amino acid residues in amyloid plaque formation and in its stability is controversial and remains under debate. This controversy is due to the fact that amyloids can be formed from nonaromatic peptides, so aromatic amino acid residues are not necessary for amyloid formation.[11]

[a]   Dr. D. B. Ninković, Dr. P. V. Petrović, Prof. Dr. E. N. Brothers, Prof.
        Dr. M. R. Belić, Prof. Dr. S. D. Zarić
        Science Program
        Texas A&M University at Qatar
        Texas A&M Engineering Building, Education City, Doha, Qatar
        E-mail: snezana.zaric@qatar.tamu.edu
[b]   D. Malenov, Prof. Dr. S. D. Zarić
        Department of Chemistry
        University of Belgrade
        Studentski trg 12-16, 11000 Belgrade, Serbia
[c]   Dr. D. B. Ninković, Dr. P. V. Petrović
        Innovation Center
        Department of Chemistry
        Studentski trg 12-16, 11000 Belgrade, Serbia
[d]   Dr. S. Niu, Prof. Dr. M. B. Hall
        Department of Chemistry
        Texas A&M University
        College Station, TX 77843-3255, USA

        Supporting information for this article can be found on:
        http:/dx.doi.org/xx.xxx/xxxxxxxxxxx

In the last few years, numerous studies have been performed on different peptides and polypeptides using various experimental and computational methods to investigate role of aromatic amino acid residues in amyloid plaque formation.[12-16] Several of these studies were performed on the Human islet amyloid polypeptide (IAPP or amylin) and its fragments. This is especially critical as the pancreatic tissues of patients affected by type 2 diabetes can contain IAPP amyloid deposits.

IAPP is a polypeptide with 37 residues containing three aromatic amino acid residues, two of Phe and one of Tyr. Formation of amyloids from IAPP polypeptides was studied using various mutants where one, two, or three aromatic amino acids were substituted with leucine.[12] The rate of amyloid formation was different for three single mutants, but all fibrils formed from single mutants were similar to fibrils formed from wild-type IAPP. The triple leucine mutant and the one of the double mutants had the slowest formation kinetics.

Results of a study on fragment 20–29 of amylin (IAPP(20–29)) indicated that the properties of aromatic amino acids that promote aggregation of peptides are a function of hydrophobicity, planar geometry, and β-sheet propensity, while formation of direct π-π interactions are not important in promoting amyloid aggregation.[14] A study on another fragment, the hIAPP(22-29) fragment, was performed on peptides with substituents that contained electron donating groups or electron withdrawing groups added to the aromatic ring of Phe-23.[15] Results show that electron donating groups on the aromatic ring of Phe-23 prevent the formation of an amyloid while peptides with electron withdrawing groups on the aromatic ring formed amyloid aggregates. Since electron donating and electron withdrawing groups on Phe-23 influence the ability of the peptide to form amyloids, but do not influence peptide hydrophobicity, it can be argued that it is not only the hydrophobic nature of the aromatic residue that is relevant in the self-assembly of hIAPP(22-29). The authors of this study thus indicated a special role for aromatic residues, although this conclusion is disputed in the studies discussed below. The experimental data also provided evidence of π-stacking in the aggregation of hIAPP(22-29).[15]

The N-terminal 12–18 region of IAPP is a highly amyloidogenic peptide with one aromatic residue (Phe) in the sequence.[13] The role of the aromatic residue Phe in amyloid aggregation was studied by substituting Phe with Leu and Ala. The results showed that substituted peptides form amyloids, indicating that aromatic Phe is not essential for amyloid aggregation. It was, however, shown that the aromatic Phe influences the kinetics of aggregation.

In addition to the studies on fragments and Human islet amyloid polypeptide (IAPP), the role of aromatic residues in amyloid formation was also studied in the amyloid β-protein (Aβ);[9] this system is believed to be involved in Alzheimer's disease. Results obtained for the amyloid β-protein (Aβ) were similar to the results for Human islet amyloid polypeptide. Specifically, the substitution of phenylalanine with leucine in the amyloid β-

FULL PAPER

protein does not significantly influence the morphology of amyloids, while it does influence the kinetics of amyloid formation.

In a recently published work[16] the role of aromatic amino acids in amyloid formation was studied by comparing the behavior of peptides with and without aromatic side chains. Results showed that naturally occurring peptides with one aromatic residue form amyloids via the same mechanism as synthetic nonaromatic peptides. Both the mechanism of the formation and the properties of the aggregates indicate that aromatic and nonaromatic residues have similar properties in this regard, and that aromatic amino acid residues are not essential for amyloid formation. However, like the results on IAPP and β-protein, this study also showed that aromatic amino acids influence the kinetics of aggregation.

It is challenging to determine the interaction energies of amyloid accumulations experimentally, while it can be done theoretically with relative ease, as quantum chemical methods are very reliable for interaction energies. Interactions of aromatic molecules have been intensively studied;[17-30] the calculated interaction energies for two known minima for the benzene dimer are -2.73 kcal mol^{-1} (for parallel stacking) and -2.84 kcal mol^{-1} (for T-shaped or edge-to-face orientation).[31] It is interesting to note that the interaction energy between benzene and aliphatic cyclohexane is stronger (-3.27 kcal mol^{-1})[32] than that between two benzene molecules; this fact is important when considering the present study.

In this work, we have studied the influence of aromatic amino acids on amyloid formation by calculating the interaction energies of peptide model systems using DFT. We have studied the interaction energies of peptides with and without aromatic side-chains. To the best of our knowledge, this is the first study of interaction energies of amyloidogenic peptides based on quantum, electronic-structure calculations.

Computational methods

All calculations were performed using the Gaussian 09 [rev. D.01] suite of programs.[33] Model systems used in the calculations were based on the crystal structures from the Protein Data Bank (PDB).[34] Hydrogen atoms were not determined by X-ray crystallography in PDB structures, thus they have been added by ArgusLab software (ver. 4.0.1).[35] All amino acids were neutralized to avoid influence of the charge in the calculations.

CCSD(T)[36-40] with complete basis set limit (CBS) calculations using Mackie's method[41] were performed on model systems created by isolating interacting side-chains of amino acids that represent typical aromatic-aromatic, aromatic-nonaromatic, and nonaromatic-nonaromatic interactions occurring in the amyloids (Figure S1, ESI). The results show that interaction energies calculated at the B3LYP-D3/6-31G*[42-47] level of theory with BSSE correction,[48] which is computationally tractable for large amyloid segments, are in good agreement with energies calculated at the CCSD(T)/CBS level (Table S1, ESI). Thus, interaction energies were calculated at B3LYP-D3/6-31G* level.

The positions of hydrogen atoms in peptides were optimized, also using the B3LYP-D3/6-31G* method. This was done because of the possible steric hindrance (bad contacts) that can be caused by hydrogens that have not been optimally positioned when placed by ArgusLab.

Results and Discussion

To contribute to understanding of amyloid β-sheets aggregation, we calculated B3LYP-D3/6-31G* interaction energies between β-sheets using model systems based on crystal structures of amyloids from the PDB. Since we wanted to study the influence of aromatic amino acids on amyloid formation, we studied both structures with aromatic amino acids in peptide sequence and structures without aromatic amino acids in the sequence. For the amyloids with aromatic amino acids, model system were based on crystal structures with PDB entry codes 2Y2A, 2Y29, 3OW9 (KLVFFA sequence)[49] and 5E5V (NFGAILS sequence)[50]., while for the amyloids without aromatic amino acids model systems were based on 2Y3J (AIIGLM sequence), 2Y3L (MVGGVVIA sequence), and 3Q2X (NKGAII sequence).[49] To calculate the interaction energies, we have extracted segments from the crystal structure that contain two tetramers of polypeptide chains. Each tetramer represents one amyloid β-sheet; monomers in tetramer are held by strong H-bonds (Figure S2, ESI). Interaction between two tetramers mimic interaction between two β-sheets in amyloids.

We calculated the total interaction energy between two β-sheets, and also partitioned this energy to account for the contribution of interactions between the side-chains of two two β-sheets, side-chains with the backbone, and between the backbones.

Because of the different sizes of the studied systems, not all of the calcualted interaction energies can be easily compared. For that reason, we have tried to scale the interaction energies using number of valence electrons.

Interaction energies between β-sheets with aromatic amino acids

We first studied peptides with both aromatic and nonaromatic side chains obtained from crystal structures 2Y2A, 2Y29, 3OW9, and 5E5V (Figure 1 and Figure S3, ESI). Structures 2Y2A, 2Y29, and 3OW9 are polymorphs with amino acid sequence KLVFFA. These structures differ in the conformation of residues side chains in the sequence (Figure S3, ESI) which causes them to form somewhat different interactions between the two tetramer β-sheets.

The 5E5V model system has a significantly stronger interaction energy of -88.69 kcal mol^{-1}, compared to the 2Y2A, 2Y29, and 3OW9 model systems with interaction energies of -40.04, -40.18, and -52.92 kcal mol^{-1} respectively (Table 1). The distances between mean planes of backbone atoms of two interacting β-sheets 7.6 Å (5E5V), 9.7 Å (3OW9), 10.0 Å (2Y29), and 10.0 Å (2Y2A) could be related to the strength of the interaction energies.

FULL PAPER

In order to understand the differences in these calculated energies, the interaction energy between two β-sheets was partitioned into various contributions from the side chains and backbone, as shown in Figure 2. Interactions between side chains can be apportioned to the contributions from aromatic-aromatic, aromatic-nonaromatic and nonaromatic-nonaromatic side chains, a division that can help to evaluate the role of aromatic amino acids on the stability of amyloids.
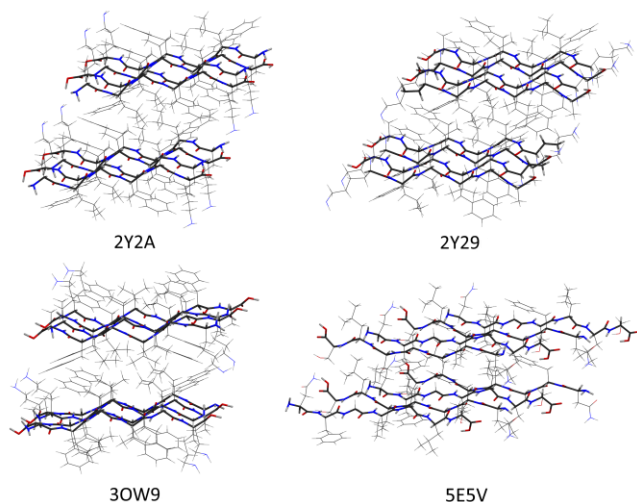

Figure 1. Model systems of two interacting tetramers, which contain both aromatic and nonaromatic residues, derived from crystal structures of peptides found in the PDB.[49, 50]
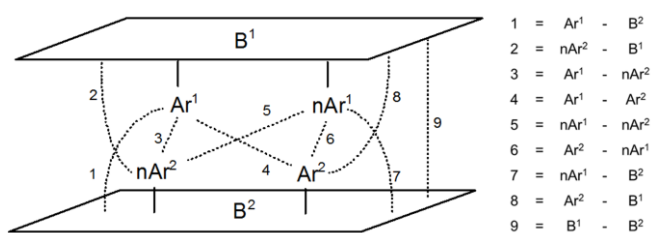

Figure 2. Schematic representation of interactions between two β-sheets. Ar – aromatic residues, nAr – nonaromatic residue, B – backbone. Interactions: Ar-Ar – interactions between aromatic side chains, Ar-nAr – interactions between aromatic and nonaromatic side chains, nAr-nAr – interactions between nonaromatic side chains, nAr-B – interactions between nonaromatic side chains and backbone, Ar-B – interactions between aromatic side chains and backbone, B-B – interactions between two backbones. Numbers in superscript represent top (^{1}) or bottom (^{2}) β-sheet

The total interaction energy can be calculated as:

$$\Delta E = \Delta E(Ar^1\text{-}Ar^2) + \Delta E(Ar^1\text{-}nAr^2) + \Delta E(Ar^2\text{-}nAr^1) + \Delta E(nAr^1\text{-}nAr^2) + \Delta E(Ar^1\text{-}B^2) + \Delta E(Ar^2\text{-}B^1) + \Delta E(nAr^1\text{-}B^2) + \Delta E(nAr^2\text{-}B^1) + \Delta E(B^1\text{-}B^2)$$

To evaluate interaction energy for aromatic-aromatic side chains, model systems were constructed by removing all nonaromatic side chains as well as backbone atoms (example of modified 2Y2A structure is given in Figure 3a).

In the case of aromatic-nonaromatic interactions, two model systems were constructed for each structure. First, a model

system was constructed by removing all aromatic amino acids in one β-sheet and all nonaromatic amino acids in the other β-sheet as well as both backbones (Figure 3b). For the second model system, the procedure was reversed, switching the roles of the two β-sheets (Figure 3c).
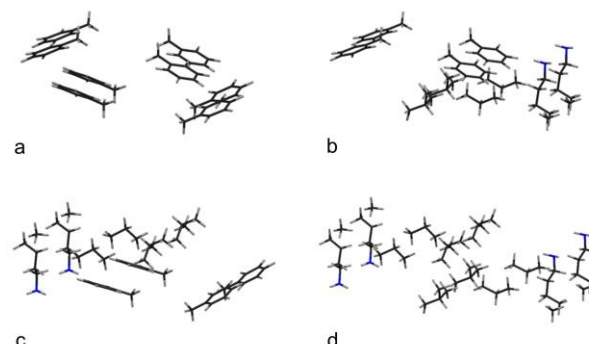

Figure 3. Example of model systems used to calculate (a) aromatic-aromatic $\Delta E(Ar\text{-}Ar)$, (b,c), aromatic-nonaromatic $\Delta E(Ar^1\text{-}nAr^2)$ and $\Delta E(Ar^2\text{-}nAr^1)$, and (d) nonaromatic-nonaromatic $\Delta E(nAr\text{-}nAr)$ interaction energies between side chains of two β-sheets in the 2Y2A structure.

For nonaromatic-nonaromatic side chain interactions, model systems were constructed by removing all aromatic side chains and backbones (Figure 3d). In similar way model systems were made to calculate contributions of backbone interactions to the total interaction energy (Figure 4), while, in all cases, broken bonds were terminated with H. Following the determination of the total interaction energies of the various components, these interaction energies will be scaled to compensate for the number of interactions in each partition.

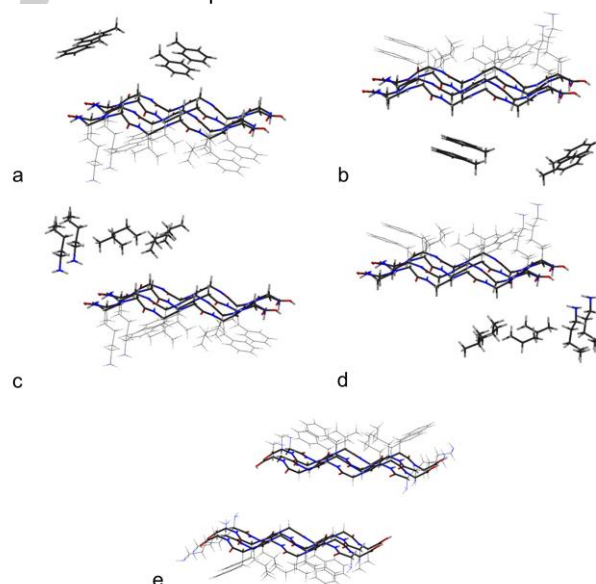**Figure 4.** Example of model systems used to calculate interaction energies of (a,b) aromatic side-chains with backbone, $\Delta E(Ar^1\text{-}B^2)$ and $\Delta E(Ar^2\text{-}B^1)$, (c,d) nonaromatic side-chains with backbones, $\Delta E(nAr^1\text{-}B^2)$ and $\Delta E(nAr^2\text{-}B^1)$, and (e) between two backbones $\Delta E(B\text{-}B)$ in the 2Y2A structure.

FULL PAPER

WILEY-VCH

Table 1. Evaluated interaction energies (in kcal mol^{-1}) and distance $R^{[a]}$ for different types of interactions[b] between two tetramer β-sheets in model systems of 2Y2A, 2Y29, 3OW9 (KLVFFA sequence), and 5E5V (NFGAILS sequence) amyloid structures

Structure	Ar-Ar	Ar^1-nAr^2	Ar^2-nAr^1	nAr-nAr	nAr^1-B^2	nAr^2-B^1	Ar^1-B^1	Ar^2-B^1	B^1-B^2	Σ	β-sheet interact.	$R^{[a]}$ (Å)
2Y2A	-11.69	-7.97	-6.21	-4.72	-2.60	-2.83	-2.81	-2.27	-1.02	-42.12	-40.04	10.0
2Y29	-10.22	-8.39	-6.84	-5.46	-2.68	-2.32	-3.20	-2.43	-0.87	-42.41	-40.18	10.0
3OW9	-9.16	-13.47	-13.47	-4.53	-3.74	-3.80	-2.89	-2.96	-1.36	-55.38	-52.92	9.7
5E5V	-2.76	-8.86	-4.2	-9.55	-12.26	-10.24	-18.02	-20.87	-7.65	-94.41	-88.69	7.6

[a] R - distance between mean planes of backbone atoms of two interacting β-sheets. [b] Interactions: Ar-Ar – aromatic-aromatic, Ar-nAr – aromatic-nonaromatic, nAr-nAr – nonaromatic–nonaromatic, nAr-B – nonaromatic-backbone, Ar-B – aromatic-backbone, B-B – backbone-backbone; suffixes in superscript designate association with one of the two interacting β-sheets; The examples of model systems for 2Y2A structure are given in Figures 3 and 4.

Data in Table 1, presenting aromatic-aromatic as well as aromatic-nonaromatic, nonaromatic-nonaromatic, and backbone interactions, enables the evaluation of the role of aromatic amino acids in the stability of four amyloid structures. As was mentioned above, model systems 2Y2A, 2Y29, and 3OW9 have the same amino acid sequence (KLVFFA), with two aromatic amino acids in the sequence, while 5E5V model system has longer amino acid sequence (NFGAILS), with only one aromatic amino acid. This difference has a major impact on the different contributions to the total interaction energy (Table 1), as it is disscused bellow in the text.

Interaction energies between side chains (ΔE(Ar-Ar), ΔE(nAr-nAr), ΔE(Ar^1-nAr^2), and ΔE(Ar^2-nAr^1)) show that the largest contribution to the total interaction energy, in all structures, comes from the aromatic-nonaromatic interactions (sum of ΔE(Ar^1-nAr^2) and ΔE(Ar^2-nAr^1)).

This contribution is largest for the 3OW9 model system, -26.94 kcal mol^{-1}, while 2Y29, 2Y2A, and 5E5V model systems have similar energies, -15.23 kcal mol^{-1}, -14.18 kcal mol^{-1}, and -13.06 kcal mol^{-1} respectively. It is interesting that for the 5E5V model system, that has only one aromatic amino acid in the sequence, aromatic-nonaromatic interactions are still stronger than other interactions between side chains.

Energies of aromatic-aromatic side chain interactions are weaker; -11.69, -10.22, -9.16, and -2.76 kcal mol^{-1} for 2Y2A, 2Y29, 3OW9, and 5E5V model systems, respectively. The very weak interaction in 5E5V model system is partially due to the fact that only one aromatic amino acid is in the sequence, and only two aromatic residues in the tetramer β-sheet oriented towards other β-sheet, hence, only two pairs of aromatic amino acids are involved in aromatic-aromatic interaction (Figure 1 and Figure S4, ESI). The distance between the centers of two interacting aromatic rings is 6.5 Å, and the angle between the planes of the rings is 45°. Large distance is another reason for the weak aromatic-aromatic interaction energy in 5E5V model system. In the other three structures there are two aromatic amino acids in the sequence, while four aromatic amino acids in β-sheet are orineted towards other β-sheet and involved in the aromatic-aromatic interactions (Figure 1 and Figure S4, ESI). Hence, in 2Y2A and 2Y29 structures, there are four pairs of interacting aromatic rings. The distances between centers of two interacting aromatic rings are 4.6 Å and 5.0 Å respectively, while

the angles between the planes of the interacting rings are 40° and 53° respectively. In 3OW9 structure, there are four pairs of interacting aromatic rings with two additional interactions of the middle rings (Figure 1 and Figure S4, ESI). The distances between the centers of two interacting aromatic rings are in the range 5.5 to 5.9 Å, while the angles are all around 45°. The distances between the centers of two interacting aromatic rings for 2Y2A, 2Y29 and 3OW9 structures are directly related to the interaction energy. Namely, shorter distances result in higher interaction energies, hence 2Y2A structure has the strongest aromatic-aromatic interaction (Table 1).

In the 2Y29, 2Y2A, and 3OW9 model systems the energies of nonaromatic-nonaromatic interactions are the weakest among side chain-side chain contributions, -5.46 kcal mol^{-1}, -4.72 kcal mol^{-1}, and -4.53 kcal mol^{-1}, respectively. Contrary to this, for the model system 5E5V, nonaromatic-nonaromatic interactions are stronger (-9.55 kcal mol^{-1}) than aromatic-aromatic interactions for this model system. This difference is mostly due to the larger number of interacting nonaromatic side chains (six nonaromatic residues in the sequence), compared to the other three structures (four nonaromatic residues in the sequence).

The backbone-backbone interaction energies are again different for 2Y2A, 2Y29, 3OW9 on one side, and 5E5V on the other side. They are not particularly strong for the 2Y2A, 2Y29, and 3OW9 (around 1 kcal mol^{-1}, Table 1), as one would anticipate, due to the large distance R, distance between the mean planes of the backbone atoms of two interacting β-sheets (around 10 Å). On the other hand, in the structure 5E5V the distance R is smaller (7.6 Å), and the interaction energy is significantly stronger, -7.65 kcal mol^{-1}.

The distance between backbones also influences the interaction energies of aromatic and nonaromatic side chains with the backbone (ΔE(Ar^1-B^2), ΔE(Ar^2-B^1), (ΔE(nAr^1-B^2), and ΔE(nAr^2-B^1)). In structures 2Y2A, 2Y29, and 3OW9 interaction energies range from -2.27 kcal mol^{-1} to -3.80 kcal mol^{-1}, while in the structure 5E5V, interaction energies are quite stronger and range from -10.24 kcal mol^{-1} to -20.87 kcal mol^{-1}. It is interesting that in the structure 5E5V, aromatic-backbone interactions are stronger than nonaromatic-backbone interactions. The presence of Gly in the structure 5E5V likely plays a role in the relatively small distance between β-sheets, and additionally contributes to

FULL PAPER

WILEY-VCH

Table 2. Evaluated interaction energies (in kcal mol^{-1}) for different types of interactions[a] between two tetramer β-sheets in model systems of 2Y3J (AIIGLM sequence), 2Y3L (MVGGVVIA sequence), and 3Q2X (NKGAII sequence)/3Q2X$_{mod}$[b] amyloid structures

Structure	nAr-nAr	nAr^1-B^2	nAr^2-B^1	B^1-B^2	Σ	β-sheet interaction	R[c] (Å)
2Y3J	6.54	-25.96	-33.67	-3.56	-56.65	-51.53	7.5
2Y3L	3.78	-23.03	-20.76	-5.50	-45.51	-42.62	7.3
3Q2X	-19.14	-71.88	-34.70	-8.35	-134.07	-125.58	7.5
3Q2X$_{mod}$	-16.49	-28.49	-29.71	-8.35	-83.04	-75.12	7.5

[a] Interactions: nAr-nAr – nonaromatic-nonaromatic, nAr-B – nonaromatic-backbone, B-B – backbone-backbone; suffixes in superscript designate association with one of the two interacting β-sheets; [b] a model system modified to remove the influence of the hydrogen bonds; [c] R - distance between mean planes of backbone atoms of two interacting β-sheets.

strong side chain-backbone interactions, since it allows close contact of side chains with backbone.

The results indicate that the aromatic-nonaromatic interactions (sum of ΔE(Ar^1-nAr^2) and ΔE(Ar^2-nAr^1)) between β-sheets are the strongest among side chain-side chain interactions in all investigated cases (Table 1). In structures with two aromatic amino acids in their sequence (2Y2A, 2Y29, and 3OW9), aromatic-aromatic interactions are stronger than nonaromatic-nonaromatic interactions, while in the structure 5E5V with one aromatic amino acid in the sequence, the aromatic-aromatic interaction is weaker (Table 1).

It is interesting to note that in spite of polar amino acids present in the sequences of all studied peptides, practically all nonaromatic interactions are interactions of aliphatic side chains. Namely, role of polar amino acids in the aromatic-nonaromatic interactions is not significant because of their position on the edge of the β-sheets (terminal position in the peptide sequence). Also, polar amino acids are not close to the backbone of the opposing β-sheet to significantly interact with it and contribute to nonaromatic-backbone interactions. As a consequence, basically all nonaromatic interactions are interactions of aliphatic side chains.

Interaction energies between β-sheets without aromatic amino acids

We also calculated interaction energies in model systems of peptides without aromatic side chains, using the 2Y3J, 2Y3L and 3Q2X structures (Figure 5, Table 2). Structures 2Y3J and 2Y3L contain only aliphatic residues, while the 3Q2X structure contains aliphatic, polar, and charged residues (Figure S5, ESI). In the 3Q2X structure, polar amino acid Asp is not involved in the interaction between two β-sheets, while neutralized Lys from one β-sheet forms H-bond with the C-terminus of the opposing β-sheet (Figure S6, ESI).

As was mentioned above, the interactions between the β-sheets containing aromatic residues have large interaction energies, i.e. in range of 40 to 89 kcal mol^{-1} (Table 1). It is very interesting that interactions between the β-sheets with only aliphatic residues are similar in strength; -51.53 kcal mol^{-1} and -42.68 kcal mol^{-1} for model systems of the 2Y3J and 2Y3L structures, respectively (Table 2). One can notice that all three of the model systems without aromatic side chains have relatively short distances between mean planes of backbone atoms of the two interacting

β-sheets, around 7.5 Å; shorter that distance for three model systems with aromatic residues, and comparable only with 5E5V structure (Table 1).

Moreover, the interaction energy in the 3Q2X structure, without aromatic residues, is exceptionally large compared to other structures, -125.58 kcal mol^{-1} (Table 2). The large interaction energy in the models of the 3Q2X structure can be a consequence of very good packing, i.e. large contact surface, and additional hydrogen bonds formed between the two β-sheets (Figure 5).
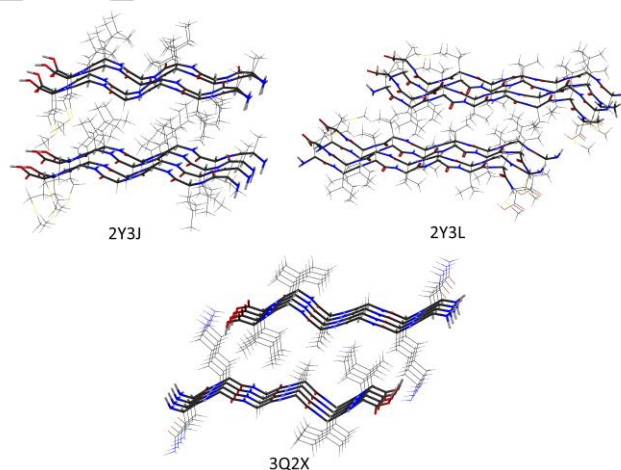

Figure 5. Model systems of two interacting tetramers which contain only nonaromatic residues, derived from crystal structures of peptides found in the PDB.[49]

In order to determine the influence of hydrogen bonds on interaction energy, the hydrogen bonds between interacting β-sheets were removed by replacing all amino groups of Lys with hydrogen atoms (Figure S6, ESI). This effectively makes this amino acid nonpolar. When the influence of the hydrogen bonds is removed, the interaction energy in the model system 3Q2X$_{mod}$ is significantly weaker, (-75.12 kcal mol^{-1}); however, it is still stronger than most of the other model systems studied in this work (Table 1 and Table 3). Since in this modified model system 3Q2X$_{mod}$ Asp is not involved in the interaction, and Lys was changed to nonpolar, interaction between two β-sheets in this model is effectively purely aliphatic-aliphatic, like in model systems 2Y3L and 2Y3J.

Table 3. Scaled interaction energies[a] (in 10^{-4} kcal mol^{-1}) for different types of interactions between two tetramer β-sheets in model systems of 2Y29, 2Y2A, 3OW9 (KLVFFA sequence), 5E5V (NFGAILS sequence), 2Y3J (AIIGLM sequence), 2Y3L (MVGGVVIA sequence), and 3Q2X (NKGAII sequence)/3Q2X$_{mod}$[b] amyloid structures

Structure		Ar-Ar	Ar^1-nAr^2	Ar^2-nAr^1	Avg (Ar-nAr)[c]	nAr-nAr
With aromatic amino acids	2Y2A	-5.64	-3.22	-2.51	-2.86	-1.60
	2Y29	-4.93	-3.39	-2.76	-3.08	-1.85
	3OW9	-4.42	-5.44	-5.44	-5.44	-1.52
	5E5V	-5.32	-2.98	-6.28	-4.63	-2.49
Without aromatic amino acids	2Y3J	-	-	-	-	1.31
	2Y3L	-	-	-	-	0.75
	3Q2X	-	-	-	-	-2.75
	3Q2X$_{mod}$	-	-	-	-	-2.86

[a] Interactions: nAr-nAr – nonaromatic-nonaromatic, nAr-B – nonaromatic-backbone, B-B – backbone-backbone; suffixes in superscript designate association with one of the two interacting β-sheets; [b] a model system modified to remove the influence of the hydrogen bonds; [c] average value for Ar^1-nAr^2 and Ar^2-nAr^1

By using the same partitioning procedure as mentioned above and bearing in mind that aromatic side chains are not present, total interaction energy between two interacting β-sheets can be calculated as:

$$\Delta E = \Delta E(nAr^1\text{-}nAr^2) + \Delta E(nAr^1\text{-}B^2) + \Delta E(nAr^2\text{-}B^1) + \Delta E(B^1\text{-}B^2)$$

Data shown in Table 2 reveals some interesting results. Namely, for the 2Y3J and 2Y3L model systems, interactions between nonaromatic (in these sequences aliphatic) side chains are repulsive (6.54 kcal mol^{-1} and 3.78 kcal mol^{-1}, respectively). This repulsive interaction is compensated by very strong interaction of side chains with backbone (nAr^1-B^2 and nAr^2-B^1; Table 2) ranging from -20.76 kcal mol^{-1} to -33.67 kcal mol^{-1}.

For the model system 3Q2X, interaction energy between nonaromatic side chains is -19.14 kcal mol^{-1}, which is the strongest amongst all nonaromatic-nonaromatic interactions calculated in this work. Interactions of nonaromatic side chains with backbones for this model system are -71.88 kcal mol^{-1} and -34.70 kcal mol^{-1}. As mentioned above, there is a sizable influence of hydrogen bonds existing in this model system. When the model system was modified to remove this influence by replacing all amino groups in Lys side chains with hydrogen atom (model 3Q2X$_{mod}$), largest change in energy can be observed for the nAr^1-B^2 interaction (from -71.88 kcal mol^{-1} to -28.49 kcal mol^{-1}; Table 2). Also, the modified model system 3Q2X$_{mod}$ gives interaction energies of nonaromatic side chains with backbone similar to those in 2Y3L and 2Y3J model systems (Table 2).

Backbone-backbone interactions (B^1-B^2) are -3.56 kcal mol^{-1}, -5.50 kcal mol^{-1}, and -8.35 kcal mol^{-1} for 2Y3J, 2Y3L, and 3Q2X/3Q2X$_{mod}$ model systems respectively.

We mentioned above that in model systems with aromatic amino acids, all nonaromatic interactions are basically aliphatic interactions. Similar, in the systems without aromatic amino

acids in two studied peptides (2Y3J, 2Y3L) all amino acids are aliphatic, while in modified 3Q2X$_{mod}$ structure all nonaromatic interactions are basically aliphatic interactions.

The data in Table 2 show that the largest contribution to the total interaction energy between two β-sheets comes from the interactions of the side-chains with the backbone. One can notice that in all studied amyloids without aromatic residues the distance between β-sheets backbones in relatively short, enabling interactions of side chains with the backbone of the other β-sheets. In addition, in all of these amyloids Gly is in the sequence, also enabling interactions of side chains with the backbone.

The experimental data on the dynamic aspects of fibril formation indicate that presence of aromatic amino acid speed up the aggregation.[15] Our data show that presence of aromatic residues change the main contribution to the total interacting energy; with aromatic residues the most important are interactions of aromatic side chains (both with other aromatic as well as with non-aromatic side chains), while without aromatic residues the most important contribution are interactions of side chains with the backbone. These data can help to explain the dynamic aspects of fibril formation. Namely, one can anticipate that the first contacts during the formation of amyloid aggregate should be the interactions between the side-chains. Hence, strong interactions between side chains can support fast formation of amyloids with aromatic amino acids.

Scaled interaction energies between β-sheets

As mentioned in the previous section, the size of interacting systems influences the value of interaction energy. To scale the energies for size, we divided the interaction energies in Table 1 and Table 2 by the product of the number of valence electrons in

the two interacting fragments. These scaled values are shown in Table 3.

It is known that noncovalent interactions depend on the electron density.[51] Since the interactions between the two β-sheets are mainly Van der Waals in nature, core electrons should not be involved in the interaction, and thus the number of interacting valence electrons would best describe the size and nature of the interactions in the interacting systems. Scaled interaction energies on an example of small aromatic molecules that supports the use of valence electron scaling method can be found in Section 3, ESI.

The scaled interaction energies between aromatic side chains are strong, with energies ranging from -4.42×10^{-4} to -5.64×10^{-4} kcal mol^{-1}. Interactions between aromatic and nonaromatic side chains (average of energies for Ar^1-nAr^2 and Ar^2-nAr^1) vary in strength, ranging from -2.86×10^{-4} to -5.44×10^{-4} kcal mol^{-1}. The scaled interactions of nonaromatic side chains are the weakest ranging from 1.31×10^{-4} to -2.86×10^{-4} kcal mol^{-1}. The strongest nonaromatic side chain interactions (for model system 3Q2X$_{mod}$), is only comparable with the weakest of interactions between aromatic and nonaromatic side chains (Table 3). As was mentioned above, nonaromatic interactions in all structures except in 3Q2X, are basically aliphatic interactions.

In the alternative way of scaling we accounted for the size of the interacting systems by dividing the interaction energies in Table 1 and Table 2 by the number of amino acids involved in the interaction between two β-sheets. The scaled interaction energies (Table S3, ESI) show the same trend as the first scaling method; the interactions between aromatic side chains are the stongest, followed with the interactions of aromatic and nonaromatic side-chains, while the interactions between nonaromatic side-chains are the weakest.

Conclusions

B3LYP-D3/6-31G* calculations were performed on interaction energies between β-sheet models for (1) amyloid model systems containing aromatic and nonaromatic amino acids and for (2) model systems without aromatic amino acids. Comparison of the calculated interaction energies for these two types of amyloids shows that most of the model systems have similar energies, independent of the presence of aromatic residues. These results support the existence of amyloid β-structures without aromatic amino acids.

For amyloids (1), with aromatic amino acids, analysis of the various contributions to total interaction energies shows that interactions of aromatic with nonaromatic (aliphatic) side chains have the largest contribution. For amyloids (2), without aromatic residues, the analysis indicates that their stability is a consequence of nonaromatic (aliphatic) side chain interactions with the backbone, while in some cases additional stabilization is achieved by hydrogen bonds.

Analysis of the scaled interactions energies show that largest side chain interaction energies are for aromatic-aromatic interactions, followed by aromatic-nonaromatic interactions, while nonaromatic-nonaromatic interactions are the weakest. However, the strength of the aromatic-nonaromatic interactions are quite similar to those of the aromatic-aromatic ones.

[1]   W. Pulawski, U. Ghoshdastider, V. Andrisano, S. Filipek, *Appl. Biochem. Biotechnol.* **2012**, *166*, 1626–1643.
[2]   E. Gazit, *FASEB J.* **2002**, *16*, 77–83.
[3]   R. Azriel, E. Gazit, *J. Biol. Chem.* **2001**, *276*, 34156–34161.
[4]   C. H. Görbitz, *Chem. Commun.* **2006**, *22*, 2332–2334.
[5]   N. R. Lee, C. J. Bowerman, B. L. Nilsson, *Biomacromolecules* **2013**, *14*, 3267–3277.
[6]   R. Qi, Y. Luo, B. Ma, R. Nussinov, G. Wei, *Biomacromolecules* **2014**, *15*, 122–131.
[7]   A. A. Profit, J. Vedad, M. Saleh, R. Z. B. Desamero, *Arch. Biochem. Biophys.* **2015**, *567*, 46–58.
[8]   M. Tena-Solsona, J. F. Miravet, B. Escude, *Chem. Eur. J.* **2014**, *20*, 1023–1031.
[9]   R. Cukalevski, B. Boland, B. Frohm, E. Thulin, D. Walsh, S. Linse, *ACS Chem. Neurosci.* **2012**, *3*, 1008−1016.
[10]   F. Bemporad, N. Taddei, M. Stefani, F. Chiti, *Protein Sci.* **2006**, *15*, 862–870.
[11]   S. M. Tracz, A. Abedini, M. Driscoll, D. P. Raleigh, *Biochemistry* **2004**, *43*, 15901–15908.
[12]   L. H. Tu, D. P. Raleigh, *Biochemistry* **2013**, *52*, 333−342.
[13]   D. Milardi, M. F. M. Sciacca, M. Pappalardo, D. M. Grasso, C. La Rosa, *Eur. Biophys. J.* **2011**, *40*, 1-12.
[14]   T. M. Doran, A. J. Kamens, N. K. Byrnes, B. L. Nilsson, *Proteins* **2012**, *80*, 1053–1065.
[15]   A. A. Profit, V. Felsen, J. Chinwong, E.-R. E. Mojica, R. Z. B. Desamero, *Proteins* **2013**, *81*, 690–703.
[16]   A. Lakshmanan, D. W. Cheong, A. Accardo, E. Di Fabrizio, C. Riekel, C. A. Hauser, *Proc. Natl. Acad. Sci. U.S.A.* **2013**, *110*, 519-524.
[17]   E. R. T. Tiekink, J. Z. Schpector, *Chem. Commun.* **2011**, 47, 6623-6625.
[18]   J. Z. Schpector, I. Haiduc, E. R.T. Tiekink, *Chem. Commun.* **2011**, *47*, 12682-12684.
[19]   a) W. B. Schweizer, J. D. Dunitz, *J. Chem. Theory Comput.* **2006**, *2*, 288-291; b) J. Řezáč, P. Hobza, *J. Chem. Theory Comput.* **2008**, *4*, 1835-1840.
[20]   a) S. Tsuzuki, K. Honda, T. Uchimaru, M. Mikami, K. Tanabe, *J. Am. Chem. Soc.* **2002**, *124*, 104-112; b) C. A. Hunter, K. R. Lawson, J. Perkins, C. J. Urch, *J. Chem. Soc. Perkin Trans. 2*, **2001**, 651-669.
[21]   M. O. Sinnokrot, E. F. Valeev, C. D. Sherrill, *J. Am. Chem. Soc.* **2002**, *124*, 10887-10893.

[22] A. Robertazzi, F. Krull, E.W. Knapp, P. Gamez, *CrystEngComm* **2011**, *13*, 3293-3300.

[23] R. K. Raju, J. W. G. Bloom, Y. An, S. E. Wheeler, *ChemPhysChem* **2011**, *12*, 3116-3130.

[24] N. A. Seifert, A. L. Steber, J. L. Neill, C. Pérez, D. P. Zaleski, B. H. Pate, A. Lesarri, *Phys. Chem. Chem. Phys.* **2013**, *15*, 11468-11477.

[25] H. Li, Y. Lu, Y. Liu, X. Zhu, H. Liu, W. Zhu, *Phys. Chem. Chem. Phys.* **2012**, *14*, 9948-9955.

[26] C. R. Martinez, B. L. Iverson, *Chem. Sci.* **2012**, *3*, 2191-2201.

[27] E. G. Hohenstein, C. D. Sherrill, *J. Phys. Chem. A* **2009**, *113*, 878-886.

[28] I. Geronimo, E. C. Lee, N. J. Singh, K. S. Kim, *J. Chem. Theory Comput.* **2010**, *6*, 1931-1934.

[29] M. Pitoňák, P. Neogrády, J. Řezáč, P. Jurecka, M. Urban, P. Hobza, *J. Chem. Theory Comput.* **2008**, *4*, 1829-1834.

[30] J. Ran, M. W. Wong, *J. Phys. Chem. A* **2006**, *110*, 9702-9709.

[31] E. C. Lee, D. Kim, P. Jurecka, P. Tarakeshwar, P. Hobza, K. S. Kim, *J. Phys. Chem. A* **2007**, *111*, 3446−3457.

[32] D. B. Ninkovic, D. Z. Vojislavljević–Vasilev, V. B. Medaković, M. B. Hall, E. N. Brothers, S. D. Zarić, *Phys. Chem. Chem. Phys.* **2016**, *18*, 25791-25795.

[33] M. J. Frisch, G. W. Trucks, H. B. Schlegel, G. E. Scuseria, M.A. Robb, J. R. Cheeseman, G. Scalmani, V. Barone, B. Mennucci, G. A. Petersson, H. Nakatsuji, M. Caricato, X. Li, H. P. Hratchian, A. F. Izmaylov, J. Bloino, G. Zheng, J. L. Sonnenberg, M. Hada, M. Ehara, K. Toyota, R. Fukuda, J. Hasegawa, M. Ishida, T. Nakajima, Y. Honda, O. Kitao, H. Nakai, T. Vreven, J. A. Jr Montgomery, J. E. Peralta, F. Ogliaro, M. Bearpark, J. J. Heyd, E. Brothers, K. N. Kudin, V. N. Staroverov, R. Kobayashi, J. Normand, K. Raghavachari, A. Rendell, J. C. Burant, S. S. Iyengar, J. Tomasi, M. Cossi, N. Rega, N. J. Millam, M. Klene, J. E. Knox, J. B. Cross, V. Bakken, C. Adamo, J. Jaramillo, R. Gomperts, R. E. Stratmann, O. Yazyev, A. J. Austin, R. Cammi, C. Pomelli, J. W. Ochterski, R. L. Martin, K. Morokuma, V. G. Zakrzewski, G. A. Voth, P. Salvador, J. J. Dannenberg, S. Dapprich, A. D. Daniels, Ö. Farkas, J. B. Foresman, J. V. Ortiz, J. Cioslowski, and D. J. Fox, Gaussian, Inc., Wallingford CT, **2009**.

[34] H. M. Berman, J. Westbrook, Z. Feng, G. Gilliland, T. N. Bhat, H. Weissig, I. N. Shindyalov, P. E. Bourne, *Nucl. Acids Res.* **2000**, *28*, 235-242,

[35] M. A. Thompson, ACS meeting, Philadelphia, **2004**, *172*, CINF 42, PA.

[36] J. Čížek, *J. Chem. Phys.* **1966**, *45*, 4256–4266.

[37] J. Čížek, J. Paldus, *Int. J. Quantum Chem.* **1971**, *5*, 359–379.

[38] J. Paldus, J. Čížek, I. Shavitt, *Phys. Rev. A: At. Mol. Opt. Phys.* **1972**, *5*, 50–67.

[39] M. Musiał, R. J. Bartlett, *Rev. Mod. Phys.* **2007**, *79*, 291–352.

[40] K. Raghavachari, G. W. Trucks, J. A. Pople, M. Head-Gordon, *Chem. Phys. Lett.* **1989**, *157*, 479–483.

[41] I. D. Mackie, G. A. di Labio, *J. Chem. Phys.* **2011**, *135*, 134318-134310.

[42] A. D. Becke, *J. Chem. Phys.* **1993**, *98*, 5648-5652.

[43] C. Lee, W. Yang, R. G. Parr, *Phys. Rev. B* **1988**, *37*, 785-789.

[44] S. Grimme, *WIREs Comput. Mol. Sci.* **2011**, *1*, 211-228.

[45] S. Grimme, J. Antony, S. Ehrlich, H. Krieg, *J. Chem. Phys.* **2010**, *132*, 154104-154119.

[46] G. A. Petersson, A. Bennett, T. G. Tensfeldt, M. A. Al-Laham, W. A. Shirley, J. Mantzaris, *J. Chem. Phys.* **1988**, *89*, 2193-218.

[47] G. A. Petersson, M. A. Al-Laham, *J. Chem. Phys.* **1991**, *94*, 6081-90.

[48] S. F. Boys, F. Bernardi, *Mol. Phys.* **1970**, *19*, 553−566.

[49] J.-P. Colletier, A. Laganowsky, M. Landau, M. Zhao, L. Goldschmidt, D. Flot, D. Cascio, M. R. Sawaya, A. B. Soriaga, D. Eisenberg, *Proc. Natl. Acad. Sci. USA* **2011**, *108*, 16938–16943.

[50] A. B. Soriaga, S. Sangwan, R. Macdonald M. R. Sawaya, D. Eisenberg, *J. Phys. Chem. B* **2016**, *120*, 5810-5816.

[51] P. Politzer, J. S. Murray, T. Clark, *J. Mol. Model*, **2015**, 21, 52.

FULL PAPER

WILEY-VCH

FULL PAPER
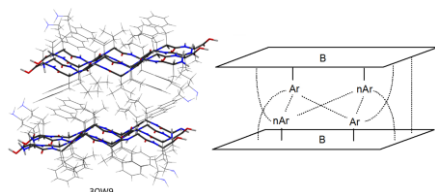
Why they stick: Aggregation of amyloid polypeptides containing aromatic and nonaromatic amino acids was studied with DFT. Interactions between side chains, and their interactions with the backbone, all play a role in the formation of amyloid plaques.

Dragan B. Ninković, Dušan P. Malenov, Predrag V. Petrović, Edward N. Brothers, Shuqiang Niu, Michael B. Hall, Milivoj R. Belić, and Snežana D. Zarić*

Page No. – Page No.

Unexpected importance of aromatic-aliphatic and aliphatic side chain-backbone interactions in the stability of amyloids